Local ensemble assimilation scheme with global constraints and conservation

Alexander Barth[(1)], Yajing Yan[(2)], Aida Alvera-Azcárate[(1)], Jean-Marie Beckers[(1)]

[(1)] GeoHydrodynamic and Environmental Research (GHER), University of Liège, Liège, Belgium

[(2)] LISTIC, Polytech Annecy-Chambéry, Université Savoie Mont-Blanc, Annecy-le-Vieux, France

September 16, 2016

Abstract

Ensemble assimilation schemes applied in their original, global formulation respect linear conservation properties if the ensemble perturbations are setup accordingly. For realistic ocean systems, only a relatively small number of ensemble members can be calculated. A localization of the ensemble increment is therefore necessary to filter out spurious long-range correlations. The conservation of the global properties will be lost if the assimilation is performed locally, since the conservation requires a coupling between all model grid points which is removed by the localization. The distribution of ocean observations is often highly inhomogeneous. Systematic errors of the observed parts of the ocean state can lead to spurious adjustment of the non-observed parts via data assimilation and thus to a spurious increase or decrease in long-term simulations of global properties which should be conserved. In this paper, we propose a local assimilation scheme (with different variants and assumptions) which can satisfy global conservation properties. The proposed scheme can also be used for non-local observation operators. Different variants of the proposed scheme are tested in an idealized model and compared to the traditional covariance localization with an ad-hoc step enforcing conservation.

It is shown that the inclusion of the conservation property reduces the total RMS error and that the presented stochastic and deterministic schemes avoiding error space rotation provide better results than the traditional covariance localization.

1 Introduction

Conservation laws are the central elements in numerical ocean modelling and for understanding the ocean dynamics in general. Key ocean variables such as mass, heat, salt and other chemical components are subject to such conservation laws. These fundamental laws allow to describe the exchange of these ocean properties and are instrumental for deriving a conceptual overview of transports in the ocean. When ocean models are developed, a significant effort is placed in maintaining the conservation laws (*e.g.* Wang et al, 2013). The ability to respect the conservation has been a strong argument in favor of numerical discretization methods like finite volumes (*e.g.* Shchepetkin and McWilliams, 2005; Madec, 2014) and a certain class of finite elements schemes (*e.g.* White et al, 2008; Danilov, 2013). On long time scales (several years), conservative numerical models are also crucial for assessing changes of physical properties, such as the total heat budget.

Global assimilation schemes can naturally satisfy global linear constraints and preserve linear conservation for suitably chosen perturbations (Janjić et al, 2014). For example, the total amount of heat is conserved by the assimilation if the temperature error introduced at every time step integrated over the whole domain is zero. When the model forecast error is only related to the uncertainty of the heat flux boundary conditions, this would mean that the integral of the flux over all open boundaries is the same for every ensemble member.

Nonlinear constraints can sometimes be transformed into linear constraints by a careful transformation of the model variables. For example, if the model variables include

sea ice concentration c_i and sea ice height h_i, then the total amount of sea ice

$$\int_\Omega c_i h_i \, \mathrm{d}x = \text{const} \tag{1}$$

is conserved without ice melting and ice formation. This conservation property is non-linear if a state vector includes c_i and h_i, but becomes linear if the state vector includes $c_i h_i$ and c_i (or h_i). For sea ice concentration and sea ice height, there is still the additional difficulty of enforcing positive quantities. But this issue is out of the scope of the present study. An approach able to conserve mass while ensuring positive quantities is discussed in Janjić et al (2014). In this method, a quadratic programming problem is solved for every ensemble member constrained by mass conservation and requiring positive values.

The need for localization arises from the fact that for realistic systems only a relatively small number of ensemble members ($\sim 10 - 1000$) can be used in general. A localization of the ensemble increment is necessary to filter out spurious long-range correlations (*e.g.* Whitaker and Hamill, 2002). However, after localization, global conservation properties of the analysis schemes are lost since the conservation requires a non-local basin-wide coupling of all model grid points which are filtered out by the localization.

One can distinguish two different localization approaches (Janjić et al, 2011; Nerger et al, 2012a): domain localization (possibly including observation localization) and covariance localization.

- In domain localization, the state vector is decomposed into sub-domains (e.g. single grid point or vertical column) where the assimilation is performed independently. Such algorithms are easily applied to parallel computers (Keppenne and Rienecker, 2003; Nerger and Hiller, 2013). To avoid discontinuities in the analysis field, this approach is combined with the observation localization (Brankart et al, 2003; Barth et al, 2007; Hunt et al, 2007). The weight of distant observations (relative to the part of the state vector to be updated) is gradually decreased by increasing the

error variance (observation localization or **R**-localization).

- For covariance localization, every single observation point is assimilated sequentially and the correction is filtered by a localization function. Because of its sequential nature, this algorithm is less suitable for parallel processing than the domain localization. This approach operates on the error covariance matrix **P** and it is sometimes called **P**-localization.

We propose an assimilation scheme which is local but can satisfy global conservation properties and can use a non-local observation operator. Both properties are indeed linked since one can introduce the global conservation as a weak constraint by using a global observation operator. The conserved property becomes thus an observed value (Pan and Wood, 2006).

The presented ensemble schemes take an ensemble as input (model forecast) and produce an ensemble as output (analysis). One recovers the original Kalman Filter analysis if the covariance does not have spurious long-range correlations. Two variants are proposed depending on whether it is required that the forecast ensemble is equal to the analysis ensemble or not, if **R** tends to infinity.

In fact, one should distinguish the cases (i) where the total amount of a given quantity is conserved but unknown and (ii) where the total amount is conserved and known without uncertainty (or with negligible uncertainty). The proposed schemes deal with the latter case.

Improving the localization schemes in the Ensemble Kalman Filter (EnKF) is an active field of research. Relatively simple analytic functions (*e.g.* Gaspari and Cohn, 1999) are often used to suppress spurious long-range correlations, and some studies (Bishop and Hodyss, 2007; Anderson, 2007; Bishop and Hodyss, 2011) highlight the benefit of using flow adaptive localization functions. Different ways to generate such adaptive localization functions have been proposed, for instance, by raising the correlation function to a given

power (Bishop and Hodyss, 2007, 2009a,b), by deriving the localization function using a smoothed-ensemble (Bishop and Hodyss, 2011) or by using a hierarchical set of ensembles (Anderson, 2007).

A difficulty similar to the conservation property is the non-local observation operator. In fact, one can represent the globally conserved quantity as a measured variable in the assimilation step. For non-local observation operators, Zhu et al (2011) have shown that by using a square root representation of the localization function, one can also derive a local assimilation scheme.

Localization can also have negative consequences on the dynamical balance (Kepert, 2009; Greybush et al, 2011). The preservation of the dynamical balance is in fact a related issue. In the same way that a conservative local analysis scheme should not change the state vector along a given direction in the error space (corresponding to the budget of the conserved quantity), one can require that the analysis increment does not increase substantially the contribution to the error sub-space defined by e.g. the ageostrohpic flow components.

This paper is organized as follows: section 2 shows the general approach to reconcile the requirements of the local assimilation method and the global conservation constraints. Different variants of the method are derived in this section. Implementation considerations are discussed in section 3 with a particular emphasis on models with a large state vector. Different variants of the proposed scheme are tested in section 4 with a univariate model and a multivariate model respectively. Conclusions and perspectives follow in section 5.

2 Method

The proposed scheme relies on a stochastic ensemble forecast

$$\mathbf{x}_{n+1}^{(k)} = \mathcal{M}\mathbf{x}_{n}^{(k)} + \eta_{n}^{(k)}, \tag{2}$$

where n is the time index of the observations, k the ensemble index ($1 \leq k \leq N$), $\mathbf{x}_n^{(k)}$ is the state vector, $\mathcal{M}$ represents the model and $\eta_n^{(k)}$ is the model error. We use the notation of Ide et al (1995) where it is appropriate. In the following, we will drop the time index n if there is no ambiguity. As the conservation properties are expressed as volume integral, such a conservation can be written as a vector product using the state vector $\mathbf{x}$:

$$\mathbf{h}^T\mathbf{x} = \text{const.} \tag{3}$$

Such an expression is directly obtained by discretizing the volume integral. The elements of $\mathbf{h}$ are areas or volumes of the corresponding grid point or zero for model variables not involved in the conservation law. We impose also that the vector $\mathbf{h}$ is normalized ($\mathbf{h}^T\mathbf{h} = 1$). Here we limit the formalism to the case where a single conservation property has to be maintained, but the equations can be generalized to multiple conservation properties where $\mathbf{h}$ becomes a matrix. Further, we assume that the model itself is conservative:

$$\mathbf{h}^T\mathcal{M}\mathbf{x} = \mathbf{h}^T\mathbf{x} \qquad \text{for all } \mathbf{x}. \tag{4}$$

In fact, $\mathbf{h}$ is an eigenvector of the adjoint of the model with an eigenvalue of 1. The stochastic perturbations should not alter the amount of the conserved quantity as mentioned before:

$$\mathbf{h}^T\eta = 0. \tag{5}$$

Also, we require that all ensemble members have the same amount of the conserved quantity initially:

$$\mathbf{h}^T\mathbf{x}_0^{(k)} = c \qquad \text{for all } k. \tag{6}$$

The ensemble covariance $\mathbf{P}$ $(n \times n)$ of this ensemble can be written in terms of its square root matrices

$$\mathbf{P} = \mathbf{S}\mathbf{S}^T, \tag{7}$$

where $\mathbf{S}$ is a matrix of size $n \times N - 1$ derived as in Hoteit et al (2002).

Given the way in which the ensemble is constructed, the uncertainty of the conserved property $\mathbf{h}^T\mathbf{x}$ is zero.

$$\mathbf{h}^T\mathbf{P}\mathbf{h} = 0 \tag{8}$$

For a localized ensemble covariance, a function (or discretized as a matrix) $\boldsymbol{\rho}$ with compact support is introduced. Spurious long-range correlations are filtered out (Hamill et al, 2001; Houtekamer and Mitchell, 2001) by using an element-wise Schur product.

$\mathbf{P}'$ is the localized ensemble error covariance.

$$\mathbf{P}' = \boldsymbol{\rho} \circ \mathbf{P} \tag{9}$$

The Schur product theorem guarantees that if the localization matrix $\boldsymbol{\rho}$ is positive semi-definite, then the product is positive semi-definite.

The localization functions substantially increase the rank of the covariance matrix by reducing the spatial coupling between the model grid points. But at the same time, any global conservation property is lost. In cases where the global conservation should be maintained, we impose a constraint on the analysis increment (for instance that the increment does not create heat or salt).

$$\mathbf{h}^T(\mathbf{x}^a - \mathbf{x}^f) = 0 \tag{10}$$

From equations (4), (5) and (6), it follows that every ensemble member perturbation

satisfies this constraint

$$\mathbf{h}^T(\mathbf{x}^{(k)} - \bar{\mathbf{x}}) = 0, \tag{11}$$

where $\bar{\mathbf{x}}$ is the ensemble mean. The error covariance is modified so that this constraint can be satisfied (Janjić et al, 2012).

$$\mathbf{P}_c = (\mathbf{I} - \mathbf{h}\mathbf{h}^T)\mathbf{P}'(\mathbf{I} - \mathbf{h}\mathbf{h}^T) \tag{12}$$

Equation (10) defines the subspace of acceptable corrections, i.e. a correction $\mathbf{x}^a - \mathbf{x}^f$ must be orthogonal to $\mathbf{h}$. Formally, one can derive the equation (12) from equation (10) by removing from every eigenvector of $\mathbf{P}'$ the contribution parallel to the vector $\mathbf{h}$.

We limit the following discussion to the case where $\mathbf{h}$ represents a conservation property, but one can also imagine to apply the current approach to enforce a dynamical balance as localization can also negatively affect the balance between the variable of the model state (Lorenc, 2003; Kepert, 2009). For instance, a geostrophic balance can be used to define the rows of a matrix $\mathbf{H}_{\text{geo}}$ corresponding to a state vector composed, among others, of sea surface height, temperature, salinity and horizontal currents. In this case, the operator $\mathbf{I} - \mathbf{H}_{\text{geo}}\mathbf{H}_{\text{geo}}^T$ would remove ageostrophic components from the error covariance.

The Kalman gain based on the modified covariance is then given by

$$\mathbf{K} = \mathbf{P}_c\mathbf{H}^T\left(\mathbf{H}\mathbf{P}_c\mathbf{H}^T + \mathbf{R}\right)^{-1}. \tag{13}$$

The product of $\mathbf{K}$ and a given vector must be computed without forming explicitly the matrix $\mathbf{P}_c$ (which has a size of $n \times n$). This is achieved by implementing the covariance matrices as operators (section 3) and by using the iterative conjugate gradient algorithm which solves a system of the form:

$$\mathbf{A}\mathbf{z} = \mathbf{b}, \tag{14}$$

where $\mathbf{A}$ is a symmetric positive-definite matrix, $\mathbf{b}$ is a given vectors in the observation space and $\mathbf{z}$ is a to be determined vector in the observation space. Here $\mathbf{A}$ is equal to $\mathbf{H}\mathbf{P}_c\mathbf{H}^T + \mathbf{R}$. For large systems, a suitable preconditioning is necessary to achieve an accurate result in an affordable number of iterations. Possible preconditioners are discussed in appendix A. Once the equation (14) is solved for a given vector $\mathbf{z}$, the product $\mathbf{K}\mathbf{b}$ is obtained by

$$\mathbf{K}\mathbf{b} = \mathbf{P}_c\mathbf{H}^T\mathbf{z}. \tag{15}$$

The mean of the analysis ensemble $\mathbf{x}^a$ can then be derived using the classical formulation:

$$\mathbf{x}^a = \mathbf{x}^f + \mathbf{K}(\mathbf{y}^o - \mathbf{H}\mathbf{x}^f), \tag{16}$$

where $\mathbf{y}^o$ is the observation vector containing m elements. The product of $\mathbf{K}$ and the innovation vector requires solving a system of m linear equations using the conjugate gradient method, as described previously. To use this approach in an ensemble forecast, one needs to derive an algorithm which is based on an ensemble as input and derives an analysis ensemble using the observations.

2.1 Stochastic analysis scheme

A stochastic analysis (Burgers et al, 1998; Houtekamer and Mitchell, 1998; Evensen, 2007) scheme can be obtained by using perturbed observations $\mathbf{y}^{o(k)}$ for every member of the ensemble $\mathbf{x}^{f(k)}$. This approach is based on equations (16) and (12), which are also used in Janjić et al (2012, 2014):

$$\mathbf{x}^{a(k)} = \mathbf{x}^{f(k)} + \mathbf{K}(\mathbf{y}^{o(k)} - \mathbf{H}\mathbf{x}^{f(k)}). \tag{17}$$

The presented approach is related to Janjić et al (2014), but it is not equivalent as

the latter allows also to maintain positive values and is based on quadratic programming which is not the case here.

The perturbations in the observations must follow a Gaussian distribution with a covariance equal to $\mathbf{R}$ for consistency (Burgers et al, 1998). This approach requires solving N independent systems of size $m \times m$. In the following, this technique is referred to as CLEnKF-Pert or LEnKF-Pert (if the conservation constraint is not used).

2.2 Deterministic analysis scheme

For small ensembles, a deterministic formulation is generally preferred to a stochastic scheme (*e.g.* Whitaker and Hamill, 2002; Nerger et al, 2005). In the following, we aim to derive a formulation without perturbed observations. Equation (17) can be rewritten as

$$\mathbf{x}^{a(k)} = (\mathbf{I} - \mathbf{KH})\mathbf{x}^{f(k)} + \mathbf{K}\mathbf{y}^{o(k)}. \tag{18}$$

As the ensemble member perturbations and the observation perturbations are independent, the error covariance matrix of $\mathbf{x}^a$ is (for any matrix $\mathbf{K}$)

$$\mathbf{P}^a = (\mathbf{I} - \mathbf{KH})\mathbf{P}^f(\mathbf{I} - \mathbf{KH})^T + \mathbf{KRK}^T, \tag{19}$$

where $\mathbf{P}^f$ is the (exact) covariance matrix of $\mathbf{x}^f$, different from $\mathbf{P}$ which is its ensemble approximation. In general, the rank of $\mathbf{P}^a$ increases, and it may even be full for a localized prior ensemble error covariance matrix. It is necessary to find some approximation to represent such an error covariance matrix using an ensemble of model states. In order to find what kind of approximations lead to a useful scheme, we temporarily assume that $\mathbf{P}^f$ in equation (19) is $\mathbf{SS}^T$ (thus not filtering spurious long-range correlations) , but the Kalman gain still uses the localized error covariance. In this case, $\mathbf{P}^a$ can be written as

$$\mathbf{P}^a = \left[\begin{array}{cc} (\mathbf{I}-\mathbf{KH})\mathbf{S} & \mathbf{KR}^{1/2} \end{array} \right] \left[\begin{array}{cc} (\mathbf{I}-\mathbf{KH})\mathbf{S} & \mathbf{KR}^{1/2} \end{array} \right]^T. \quad (20)$$

The first part of the expression in the brackets ($(\mathbf{I}-\mathbf{KH})\mathbf{S}$, N columns) corresponds to the model forecast error expressed as the forecast ensemble modified by the Kalman gain and the second part ($\mathbf{KR}^{1/2}$, m columns) represents the error increase due to the uncertainty in the observations. The latter $N+m$ columns can be used to create an ensemble with appropriate covariance. Clearly the number of ensemble members should not increase in every analysis cycle. If very few observations are used, the expression in brackets can be reduced by using a singular value decomposition (SVD) and keeping only the leading singular vectors and singular values. However, for a large number of observations (e.g. satellite observations), this approach can be prohibitive. Otherwise, we can try to project the term due to uncertain observations into some error space. A reasonable choice is

$$\mathbf{S}' = (\mathbf{I}-\mathbf{KH})\mathbf{S}, \quad (21)$$

as this error space is derived from the dominant model forecast error modes (equation 20). These error modes also satisfy the defined constraint:

$$\mathbf{h}^T\mathbf{S}' = 0 \quad \text{since } \mathbf{h}^T\mathbf{S} = 0.$$

In general, the columns of $\mathbf{S}$ are not an orthogonal basis. A vector can be constrained to the subspace defined by the columns of $\mathbf{S}$ by multiplying the vector with the matrix $\mathbf{S}'\left(\mathbf{S}'^T\mathbf{S}'\right)^{-1}\mathbf{S}'^T$. The covariance matrix $\mathbf{P}^a$ is then projected onto the subspace determined by the columns of $\mathbf{S}$. The projected matrix $\mathbf{P}^a_{S'}$ and the full covariance matrix are related by

$$\mathbf{P}^a_{S'} = \mathbf{S}'^T \mathbf{P}^a \mathbf{S}' \tag{22}$$

$$\mathbf{P}^a = \mathbf{S}' \left(\mathbf{S}'^T \mathbf{S}'\right)^{-1} \mathbf{P}^a_{S'} \left(\mathbf{S}'^T \mathbf{S}'\right)^{-1} \mathbf{S}'^T + \text{contrib. in perp. space to be neglected} \tag{23}$$

Using equation (19) and the conservative and localized error covariance matrix $\mathbf{P}_c$, one obtains the following expression for $\mathbf{P}^a_{S'}$:

$$\mathbf{P}^a_{S'} = (\mathbf{S}'^T - \mathbf{S}'^T \mathbf{K}\mathbf{H}) \mathbf{P}_c (\mathbf{S}'^T - \mathbf{S}'^T \mathbf{K}\mathbf{H})^T + \mathbf{S}'^T \mathbf{K}\mathbf{R}\mathbf{K}^T \mathbf{S}'. \tag{24}$$

The product $\mathbf{K}^T \mathbf{S}'$ is also computed using the conjugate gradient algorithm.

$$\mathbf{K}^T \mathbf{S}' = \left(\mathbf{H}\mathbf{P}_c\mathbf{H}^T + \mathbf{R}\right)^{-1} \mathbf{H}\mathbf{P}_c\mathbf{S}' \tag{25}$$

Section 3 will describe in more detail how this can be done efficiently.

Finally, one gets the following expression of a square root of the matrix $\mathbf{P}^a = \mathbf{S}^a \mathbf{S}^{aT}$:

$$\mathbf{S}^a = \mathbf{S}' \left(\mathbf{S}'^T \mathbf{S}'\right)^{-1} (\mathbf{P}^a_{S'})^{1/2}, \tag{26}$$

where $(\mathbf{P}^a_{S'})^{1/2}$ is the principal square root of $\mathbf{P}^a_{S'}$ which is unique and can be computed by an eigenvector decomposition.

This approach requires solving $2(N-1)$ systems of size $m \times m$ for the error modes and one system for the ensemble mean. The N systems are in fact independent and can be distributed on a parallel machine.

Based on the ensemble mean $\mathbf{x}^a$ and the error modes $\mathbf{S}^a$, one can reconstruct an ensemble. The procedure is explained in Hoteit et al (2002), but we choose not to use the optional random rotation matrix mentioned in this study, because it tended to degrade the results. We will refer to this technique as CLEnKF-$\mathbf{P}_c$ or LEnKF-$\mathbf{P}_c$ (if the conservation

constraint is not used).

2.3 Deterministic analysis scheme avoiding rotation of the ensemble

Even when the observation error variances are much larger than the model forecast error variances (and in the limit as $\mathbf{R}$ goes to infinity), the analysis ensemble is different from the forecast ensemble, even if the mean and covariance are unchanged. This is because $\mathbf{P}^a_{S'}$ tends to $\mathbf{S}^T\mathbf{P}_c\mathbf{S}$, and the principal square root of this matrix introduces a rotation which should be avoided (Nerger et al, 2012b). Therefore, we want that $\mathbf{P}^a_{S'}$ tends to the following:

$$\mathbf{P}^a_{S'} \rightarrow \mathbf{S}^T\mathbf{S}\mathbf{S}^T\mathbf{S}, \tag{27}$$

so that the principal square root of $\mathbf{P}^a_{S'}$ tends to $\mathbf{S}^T\mathbf{S}$ (because it is unique) and $\mathbf{S}^a$ will tend to $\mathbf{S}$. This can be achieved by modifying equation (24), so that this equation reads

$$\mathbf{S}'^T\mathbf{P}^a\mathbf{S}' \;=\; \mathbf{S}'^T\mathbf{S}'\mathbf{S}'^T\mathbf{S}' + \mathbf{S}'^T\mathbf{K}\mathbf{R}\mathbf{K}^T\mathbf{S}'. \tag{28}$$

If $\mathbf{R}$ tends to $+\infty$, the Kalman gain tends to zero and equation (28) becomes

$$\mathbf{S}^a \rightarrow \mathbf{S}'\left(\mathbf{S}'^T\mathbf{S}'\right)^{-1}\mathbf{S}^T\mathbf{S} = \mathbf{S}. \tag{29}$$

and the analysis ensemble will be exactly the forecast ensemble. But it should be clear that this assimilation scheme requires an additional approximation. In the following experiments, we will test if this approximation (using the ensemble covariance in equation (28)) outweighs the benefit of avoiding an unnecessary rotation of the ensemble space. This technique will be referred to as CLEnKF-$\mathbf{S}\mathbf{S}^T$ or LEnKF-$\mathbf{S}\mathbf{S}^T$ (whether the

conservation constraint is not used).

3 Implementation

The localization function is implemented as a function returning the indices and values of the non-zero elements for a given row of the localization matrix $\boldsymbol{\rho}$. A fast implementation of this routine is crucial for large implementations. For a regularly structured grid, it is possible to compute the indices close to a given point efficiently without iteration over all model grid points. For an unstructured grid, efficient algorithms have also been proposed (*e.g.* Löhner and Ambrosiano, 1990) whose cost depends essentially on the logarithm of the number of grid points.

The matrices $\mathbf{P}'$ and $\mathbf{P}_c$ are not implemented as $n \times n$ arrays, but as operators acting on a given vector $\mathbf{x}$:

$$\mathbf{P}'\mathbf{x} = (\boldsymbol{\rho} \circ \mathbf{S}\mathbf{S}^T)\mathbf{x}.$$

To compute this product, one needs to leverage the fact that every row of the localization matrix $\boldsymbol{\rho}$ has a relatively small number of nonzero elements (compared to its size n). For every element of the vector $\mathbf{P}'\mathbf{x}$, only the elements of $\mathbf{S}\mathbf{S}^T$ are computed for which the corresponding of $\boldsymbol{\rho}$ is nonzero. The computation of the product $\mathbf{P}'\mathbf{x}$ takes thus $\mathcal{O}(n\, n_{\text{loc}}\, N)$ operations where n_{loc} is the number of nonzero elements returned by the localization function used to build the localization matrix $\boldsymbol{\rho}$. To compute the product of $\mathbf{P}_c$ and a given vector $\mathbf{x}$, one needs to involve in addition the projection operator $\mathbf{I} - \mathbf{h}\mathbf{h}^T$. This is a fast operation which does not have any significant impact on the order of magnitude of the number of operations.

At different stages of the algorithm (equations (21), (17), (25)), the following system needs to be solved for $\mathbf{z}$ for a given right-hand side vector $\mathbf{b}$:

$$\left[\mathbf{H}(\mathbf{I} - \mathbf{h}\mathbf{h}^T)\mathbf{P}'(\mathbf{I} - \mathbf{h}\mathbf{h}^T)\mathbf{H}^T + \mathbf{R}\right]\mathbf{z} = \mathbf{b} \tag{30}$$

We use the conjugate gradient algorithm which requires the repeated application of the matrix in brackets to a given vector. For simple expressions of the observation error covariance matrix, such as a diagonal matrix, a matrix decomposed in its square roots or a sum of a diagonal matrix and a product of square root matrix (Brankart et al, 2009), efficient ways to handle the observation error covariance matrix exist. However, the application of the localized model error covariance matrix in the observation space to the vector $\mathbf{z}$, might be more difficult to compute. By expanding this product, we obtain the following terms:

$$\mathbf{H}\mathbf{P}'\mathbf{H}^T\mathbf{z} - \mathbf{H}\mathbf{h}\mathbf{a}^T\mathbf{H}^T\mathbf{z} - \mathbf{H}\mathbf{a}\mathbf{h}^T\mathbf{H}^T\mathbf{z} + \mathbf{H}\mathbf{h}\mathbf{h}^T\mathbf{a}\mathbf{h}^T\mathbf{H}^T\mathbf{z} + \mathbf{R}\mathbf{z} = \mathbf{b}, \tag{31}$$

where we can define and pre-compute the vector $\mathbf{a} = \mathbf{P}'\mathbf{h}$. This vector corresponds to the covariance of the conserved quantity with all elements of the state vector (based on the localized covariance matrix).

All terms of equation (31) can be computed in a straight-forward and efficient way, except the product of $\mathbf{H}(\boldsymbol{\rho} \circ \mathbf{S}\mathbf{S}^T)\mathbf{H}^T$ and a vector $\mathbf{z}$. In some implementations of covariance localization, this matrix is approximated by changing the order of operations and applying the localization in observation space (Hamill et al, 2001). However, if $\mathbf{H}$ is sparse, there is no need to compute all non-zero elements $\boldsymbol{\rho} \circ \mathbf{S}\mathbf{S}^T$. In fact, it is sufficient to compute only those who are later multiplied by the non-zero values of $\mathbf{H}$. The number of operations for a single vector increases thus only linearly with the number of observations m and the number of nonzero elements returned by the localization functions (noted n_{loc}).

The number of operations of the overall method is determined by the number of iterations N_{iter} necessary to reach convergence. As the conjugate gradient method has to be applied for all ensemble members, the total number of operations is $\mathcal{O}(n\, n_{\mathrm{loc}}\, N^2\, N_{\mathrm{iter}} + m\, N\, N_{\mathrm{iter}} + m\, n\, N_{\mathrm{iter}})$ (including only terms proportional to N_{iter}). Here we assumed the

favorable but common case of a diagonal observational error covariance matrix and that the observation operator represents an interpolation (which can thus be represented by a sparse matrix with an order of m nonzero elements).

4 Results

4.1 Assimilation setup

The assimilation setup is based on a classical twin experiment using the Kuramoto-Sivashinsky equation (section 4.2) and a minimal model for sea ice and salinity with conservation (section 4.3). For all assimilation experiments, the localization length scale and inflation factors are varied to obtain the optimal values of these parameters as in Nerger et al (2012a). The inflation factor is constant over the domain and applied to the a posteriori error covariance.

The following test cases are performed:

- CL: standard covariance localization: observations are assimilated sequentially with the ETKF (Bishop et al, 2001; Nerger, 2015) and the correction is multiplied by a localization function.
- CL-adj: The same as CL, but after the analysis, the budget is corrected with an adjustment step by adding or removing a spatially constant term to all model grid points.
- LEnKF-pert: Localized EnKF using perturbed observations without conservation constraint (section 2.1, implementing equations (13) and (17) with $\mathbf{P}_c = \mathbf{P}'$).
- CLEnKF-pert: Localized EnKF using perturbed observations with conservation constraint (section 2.1, implementing equations (13) and (17)).

- LEnKF-$\mathbf{P}_c$: Localized EnKF variant "$\mathbf{P}_c$" without conservation constraint (section 2.2, implementing equations (13), (24) and (26) with $\mathbf{P}_c = \mathbf{P}'$).

- CLEnKF-$\mathbf{P}_c$: Localized EnKF variant "$\mathbf{P}_c$" with conservation constraint (section 2.2, implementing equations (13), (24) and (26)).

- LEnKF-$\mathbf{SS}^T$: Localized EnKF variant "$\mathbf{SS}^T$" without conservation constraint (section 2.3, implementing equations (13), (28) and (26) with $\mathbf{P}_c = \mathbf{P}'$).

- CLEnKF-$\mathbf{SS}^T$: Localized EnKF variant "$\mathbf{SS}^T$" with conservation constraint (section 2.3, implementing equations (13), (28) and (26)).

4.2 Kuramoto-Sivashinsky equation

We want to test the proposed assimilation scheme with a chaotic system which exhibits naturally a conserved quantity. This is the case of the Kuramoto-Sivashinsky system (*e.g.* Khellat and Vasegh, 2014) which is governed by the equation

$$\frac{\partial v}{\partial t} = -\frac{\partial^2 v}{\partial x^2} - \frac{\partial^4 v}{\partial x^4} - v\frac{\partial v}{\partial x}, \tag{32}$$

over a periodic domain Ω whose length is usually set to $L = 32\pi$. Figure 1 illustrates the solution of the Kuramoto-Sivashinsky system (without assimilation). By writing the previous equation in flux form, one can show that the quantity v integrated over the domain does not change over time:

$$\frac{d}{dt}\int_\Omega v \, \mathrm{d}x = 0. \tag{33}$$

This conservation property is used in the proposed assimilation scheme. The domain is discretised with 128 grid points. The time step is $\Delta t = 1/4$ and the ETDRK4 discretisation scheme (Exponential Time Differencing fourth-order Runge-Kutta) is used (Cox and Matthews, 2002). The discretized model also respects the equation (33).

The initial condition of the free-running simulation is given by

$$v(x) \quad = \quad \cos\left(\frac{x}{16}\right)\left(1+\sin\left(\frac{x}{16}\right)\right). \tag{34}$$

As localization function, a compactly supported 5th-order piece-wise rational function from Gaspari and Cohn (1999) is used and its expression is given by

$$f(r) = \begin{cases} -\frac{1}{4}r^5 + \frac{1}{2}r^4 + \frac{5}{8}r^3 - \frac{5}{3}r^2 + 1, & \text{if } r \leq 1 \\ \frac{1}{12}r^5 - \frac{1}{2}r^4 + \frac{5}{8}r^3 + \frac{5}{3}r^2 - 5r + 4 - \frac{2}{3r}, & \text{if } r \leq 2 \\ 0, & \text{if } r > 2, \end{cases} \tag{35}$$

where r is the distance scaled by a given length-scale L.

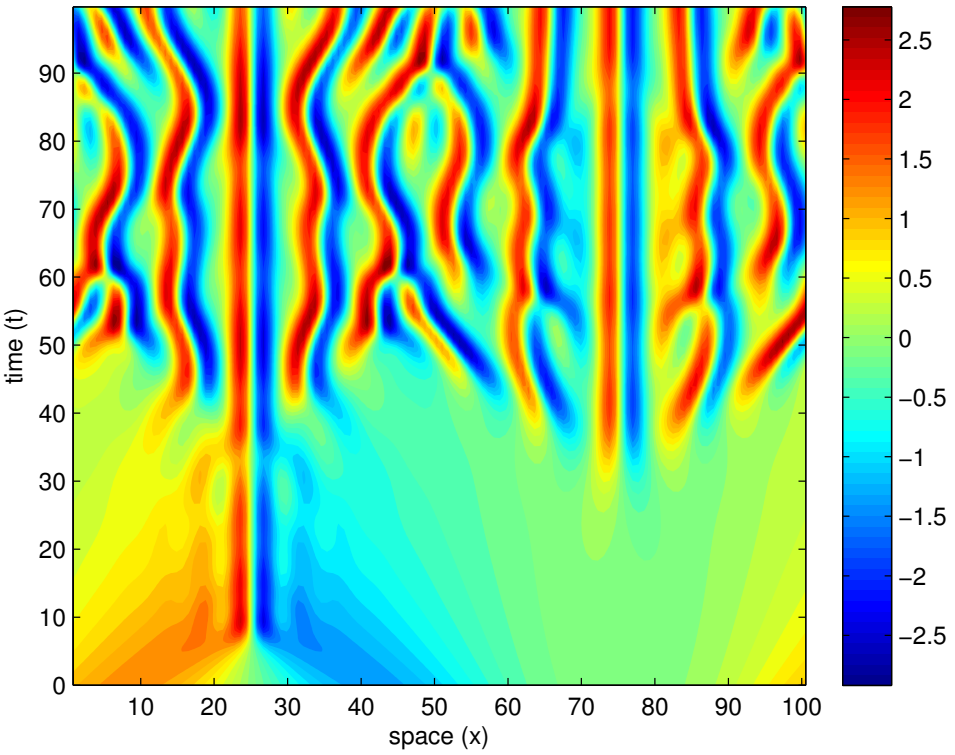

Figure 1: Solution of the Kuramoto-Sivashinsky equation (without assimilation).

Every 8th grid point is observed (with an error variance of 0.1) at every 10 model time steps. The model is run in total for 1000 time steps and the experiment is repeated 1000 times. The RMS errors relative to the true solution are averaged. As the system

has only 128 grid points, a relatively small ensemble of 30 members is used. The error in the initial condition is generated by

$$\mathbf{x}_0^{(k)} = \mathbf{x}_{\text{free}}^{(k)} + (\mathbf{I} - \mathbf{h}\mathbf{h}^T)\mathbf{P}_i{}^{1/2}\mathbf{z}^{(k)}, \tag{36}$$

where $\mathbf{P}_i$ is a diagonal matrix with diagonal elements equal to 0.1. Therefore, the added perturbation does not modify the total budget. A similar perturbation is generated for the "truth" run and for the error introduced at every time step (with a variance of 10^{-7} before its spatial average is subtracted).

Figure 2 illustrates the results of the model state vector at the location $x = 0$ (where observations are available). The results correspond to the assimilation method "CLENKF-$\mathbf{P}_c$" with an inflation factor of 1.05 and a localization length scale of 25 grid points. The blue curve corresponds to the true model solution and the black line represents a free model run (with perturbed initial conditions and model noise added at every time step). From the true model solution, observations are extracted and perturbed (green dots) and assimilated in the ensemble model run. The black segments on Figure 2 correspond to the ensemble forecast where the starting point is the analysis and the end point is the forecast of the next analysis cycle. In most circumstances the ensemble can track the true model state reasonably well. The largest discrepancy between the ensemble mean and the true state is observed at time step 209. The individual ensemble members (in light-gray) strongly diverge at this time instance, which reflects a low predictability. It is not expected that the ensemble converges to the true solution because the model dynamics are chaotic and because random perturbations are added at every time step.

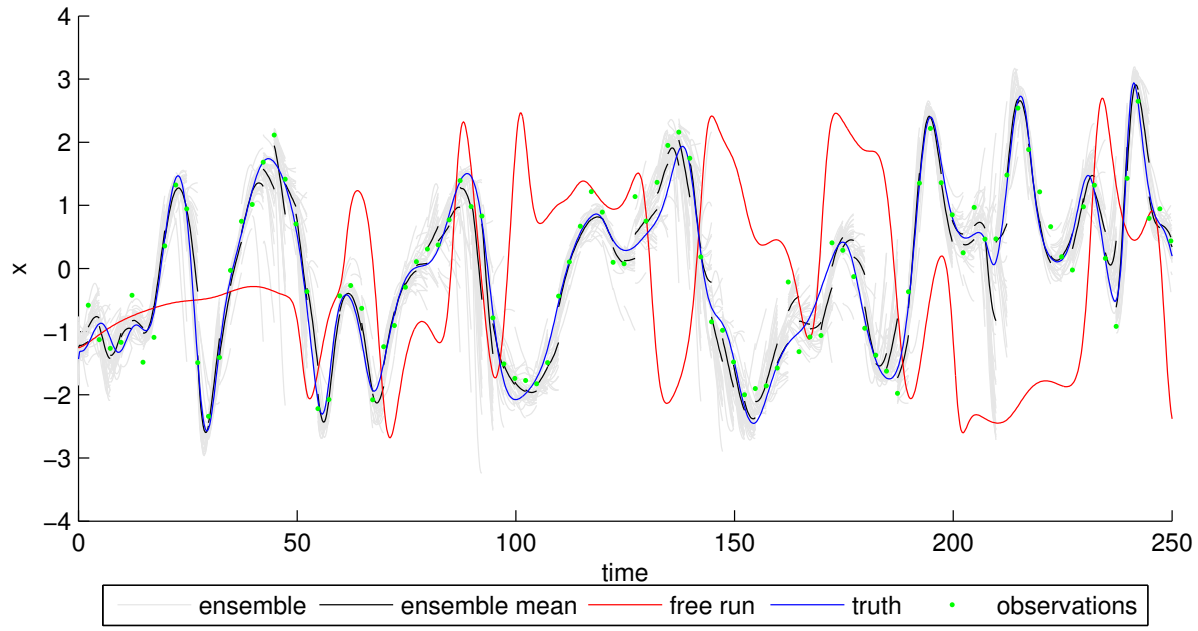

Figure 2: Example of the twin experiment simulation at $x = 0$ as a function of time (one time unit corresponds to 4 time steps) using the assimilation method "CLENKF-$\mathbf{P}_c$" with an inflation factor of 1.05 and a localization length scale of 25 grid points.

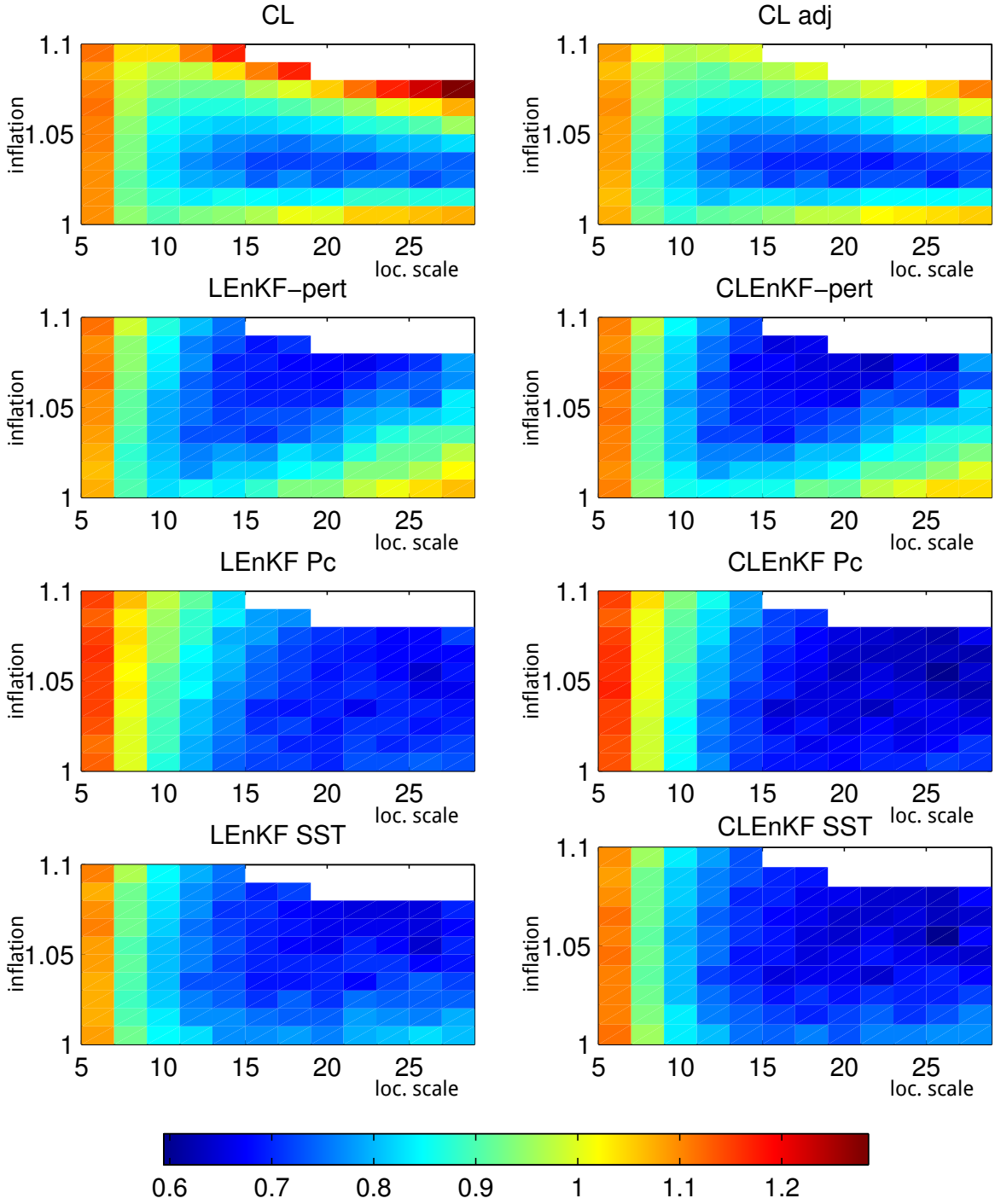

Figure 3: RMS error between the model run with assimilation and the true solution for different schemes and parameters. The x-axis represents the localization length-scale and the y-axis the inflation factor.

Table 1: The lowest RMS error for different assimilation schemes and the corresponding parameters. The last column represents the standard deviation of the RMS error averaged over all tests. It is computed as the standard deviation of all RMS errors divided by the square root of the number of tests. The lowest RMS error among the different schemes is in bold.

	L	inflation	mean RMS	std of mean RMS
CL	21	1.03	0.71375	0.00271
CL-adj	21	1.03	0.68624	0.00268
LEnKF-pert	21	1.07	0.66267	0.00570
CLEnKF-pert	21	1.07	0.63493	0.00609
LEnKF $\mathbf{P}_c$	25	1.05	0.64253	0.00364
CLEnKF $\mathbf{P}_c$	25	1.05	**0.59395**	0.00386
LEnKF $\mathbf{S}\mathbf{S}^T$	25	1.05	0.64078	0.00513
CLEnKF $\mathbf{S}\mathbf{S}^T$	25	1.05	0.59953	0.00452

Figure 3 shows the RMS error model run with assimilation and the true solution for different schemes and different values of the localization length-scale and the inflation factor. White areas in Figure 3 with standard covariance localization represent model parameters where the system becomes unstable. The optimal parameter configuration is reported in Table 1 with the corresponding RMS error. Covariance localization with the "ad-hoc" adjustment (CL-adj) provides only very small improvement compared to the classical covariance localization scheme (CL). In both cases, the optimal correlation length and inflation factor are 21 grid points and 1.03 respectively. The resulting RMS error of these experiments is more sensitive to changes in the inflation factor than to the localization length-scale (for the range of tested parameters). A good choice of the inflation factor is thus quite important as the "valley" (panel CL and CL-adj of Figure 3) is relatively narrow. One obtains consistently better results when the conservation property is explicitly used than without this constraint.

The new local assimilation schemes provide a lower RMS error in these twin experiments. However, to reach the optimal RMS error, a slightly larger inflation factor than in the classical scheme was necessary. For an inflation equal to 1.03, the stochastic schemes provided indeed worse results than the ETKF with covariance localization and adjustment (CL-adj). We attribute this to the fact that for relatively small ensemble sizes, the

statistical fluctuations are large and that a deterministic scheme provides better results. However, even for an inflation equal to 1.03 the new deterministic scheme provides lower RMS errors than in the experiment CL-adj.

Overall, the performance of the four new schemes (LEnKF-$\mathbf{P}_c$, CLEnKF-$\mathbf{P}_c$, LEnKF-$\mathbf{S}\mathbf{S}^T$, CLEnKF-$\mathbf{S}\mathbf{S}^T$) is relatively similar. It is interesting to note that the sensitivity of the RMS error relative to the inflation factor is much lower compared to the cases CL and CL-adj. In fact, one would even obtain acceptable results without any inflation at all for the schemes LEnKF $\mathbf{P}_c$ and CLEnKF $\mathbf{P}_c$ with the present model.

The lowest error was obtained with the scheme CLEnKF $\mathbf{P}_c$ enforcing the conservation and using the localized error covariance to derive the updated ensemble members.

Since the serial observation processing can have a detrimental effect on the results (Nerger, 2015), we repeated the setup of the case LEnKF-pert followed by the adjustment step as in experiment CL-adj for an inflation factor of 1.07 and localization length of 21. As for the Kuramoto-Sivashinsky model, the optimal values of the inflation factor and the length-scale were not sensitive to whether the conservation was enforced or not. The mean RMS error compared to the true run was 0.66072 which represents only a slightly RMS reduction. Given the standard deviation of the mean RMS is 0.00498, one cannot claim the adjustment step has a significant impact on the improvement of the realism of the model.

4.3 Minimal model for sea ice and salinity with conservation

The previous test presented the results for a conservative univariate model. However, the conservation property involves sometimes multiple model variables. For instance, in a coupled sea-ice and hydrodynamic model the amount of total salt is conserved. We look for minimal model for sea-ice and salinity with this conservation property. In this system, the integral of a function $f(\phi_1, \phi_2, \dots)$ of the model variables $\phi_1, \phi_2, \dots$ over a

closed domain remains constant over time:

$$\frac{d}{dt}\int_{\Omega} f(\phi_1(x), \phi_2(x), \dots)\, \mathrm{d}x = 0. \tag{37}$$

We use a simple multivariate model which mimics the coupling between a sea-ice model and a hydrodynamic model. The advection velocity (v) is essentially provided using the Kuramoto-Sivashinsky equation. The flow v is "compressible" as it varies with x. Thus we use also the variable h, representing the height of the layer, governed by the continuity equation.

$$\frac{\partial h}{\partial t} + \frac{\partial hv}{\partial x} = 0 \tag{38}$$

It was necessary to add a pressure gradient term ($-g\frac{\partial h}{\partial x}$) to the Kuramoto-Sivashinsky equation in order to prevent an unrealistic variability of the layer thickness. This feedback term prevents an excessive increase or decrease in the layer thickness. It makes the system behave more like a shallow-water model but it still exhibits chaotic behavior.

$$\frac{\partial v}{\partial t} = -\frac{\partial^2 v}{\partial x^2} - \frac{\partial^4 v}{\partial x^4} - v\frac{\partial v}{\partial x} - g\frac{\partial h}{\partial x} \tag{39}$$

The salinity (S) is governed by the following equation which includes an advection term, a diffusion term and a source and sink term $\mu\mathcal{F}(t)$.

$$\frac{\partial hS}{\partial t} + \frac{\partial vhS}{\partial x} = \kappa\frac{\partial^2 hS}{\partial x^2} + \mu\mathcal{F}(t) \tag{40}$$

The dynamics of the ice concentration (c) are given by advection (including an addi-

tional ice-drift) and the source and sink term:

$$\frac{\partial c}{\partial t} + \frac{\partial (v_c + v)c}{\partial x} = \mathcal{F}(t). \tag{41}$$

The additional drift v_c of the sea ice is set to a constant. The term $\mathcal{F}$ represents the exchanges between sea ice and salinity. Here it is represented by a sinusoidal function (representing seasonal melting and ice formation):

$$\mathcal{F}(t) = A_{\mathcal{F}} \sin\left(\omega_{\mathcal{F}} t\right).$$

The values of all model parameters are given in Table 2. Equation (40) can be rewritten in conservative form as

$$\begin{aligned} \frac{\partial hS}{\partial t} + \frac{\partial F_S}{\partial x} &= \mu \mathcal{F} && (42)\\ \frac{\partial c}{\partial t} + \frac{\partial (v_c + v)c}{\partial x} &= \mathcal{F}, && (43)\\ & && (44) \end{aligned}$$

where the flux F_S is defined by

$$F_S = vhS - \kappa \frac{\partial hS}{\partial x}. \tag{45}$$

For a periodic domain Ω, salinity fluxes and ice fluxes mutually cancel after integration over the whole domain and one obtains the following conservation property:

$$\frac{d}{dt} \int_\Omega (hS - \mu c)\, dx = 0. \tag{46}$$

It involves a product between the thickness h and the salinity S. It is thus nonlinear in these variables. The problem is circumvented as mentioned in section 1 by using the

product hS as variable in the state vector (along with h, c and v). It is not necessary to compute the salinity S as the model equations are expressed directly in terms of hS. The equations are discretised in such a way that the conservation expressed in equation (46) is respected. For completeness, we also provide the initial conditions of the unperturbed simulation:

$$v = \cos\left(\frac{x}{16}\right)\left(1+\sin\left(\frac{x}{16}\right)\right), \tag{47}$$

$$hS = \cos\left(\frac{x}{16}\right)\left(1+\sin\left(\frac{x}{16}\right)\right), \tag{48}$$

$$h = 20, \tag{49}$$

$$c = \exp\left(\frac{-(x-16\pi)^2}{(5/4\pi)^2}\right). \tag{50}$$

The results of this simulation are illustrated in Figure 4. The solution is strongly dominated by the chaotic behavior of the velocity equation. Given the present observation technology, we decided to observe every second ice concentration grid point. All other model variables, in particular salinity, are not observed. At every time step, a random error is introduced. It is drawn from a random Gaussian distribution without spatial correlation and with an error variance of 10^{-7}. The total amount of salt is set to zero before applying the model error to the state vector.

The assimilation experiment has been repeated 1000 times for different realizations of the initial conditions and model error and for different values of the correlation length and inflation factor. For each simulation, the RMS error relative to the true solution has been calculated. The RMS errors are presented in Figure 5 and synthesized in Table 3.

The results of Figure 5 appear noisy but even after increasing the number of experiments, these small-scale variations remained and were stable as it can also be seen by the low standard deviation of the mean RMS error (last column of Table 3). In the experiments of section 4.2, the assimilation experiments with explicitly enforced conservation always improved the total mean RMS error (Table 3). It should be noted, however, that

the schemes LEnKF-$\mathbf{P}_c$ and CLEnKF-$\mathbf{P}_c$ provided worse results than the classical covariance localization schemes. We attribute this result to the fact that these schemes, unlike other tested schemes, introduce a possible rotation of the error space (even when $\mathbf{R}$ tends to infinity). For the multivariate model, this detrimental effect outweighs the possible benefits of enforcing the conservation. The best results were obtained with the schemes where this rotation is avoided.

Table 2: Model parameters for the coupled multivariate model.

Parameter	Value	Interpretation
L	2π	length of the domain
g	0.1	acceleration due to gravity
v_c	2	additional drift of sea ice
Δt	0.1	time step
$A_{\mathcal{F}}$	$\frac{1}{100}$	amplitude of the melting-freezing cycle
$\omega_{\mathcal{F}}$	$\frac{1}{10}$	angular frequency of sea melting-freezing cycle
κ	0.08	diffusion coefficient

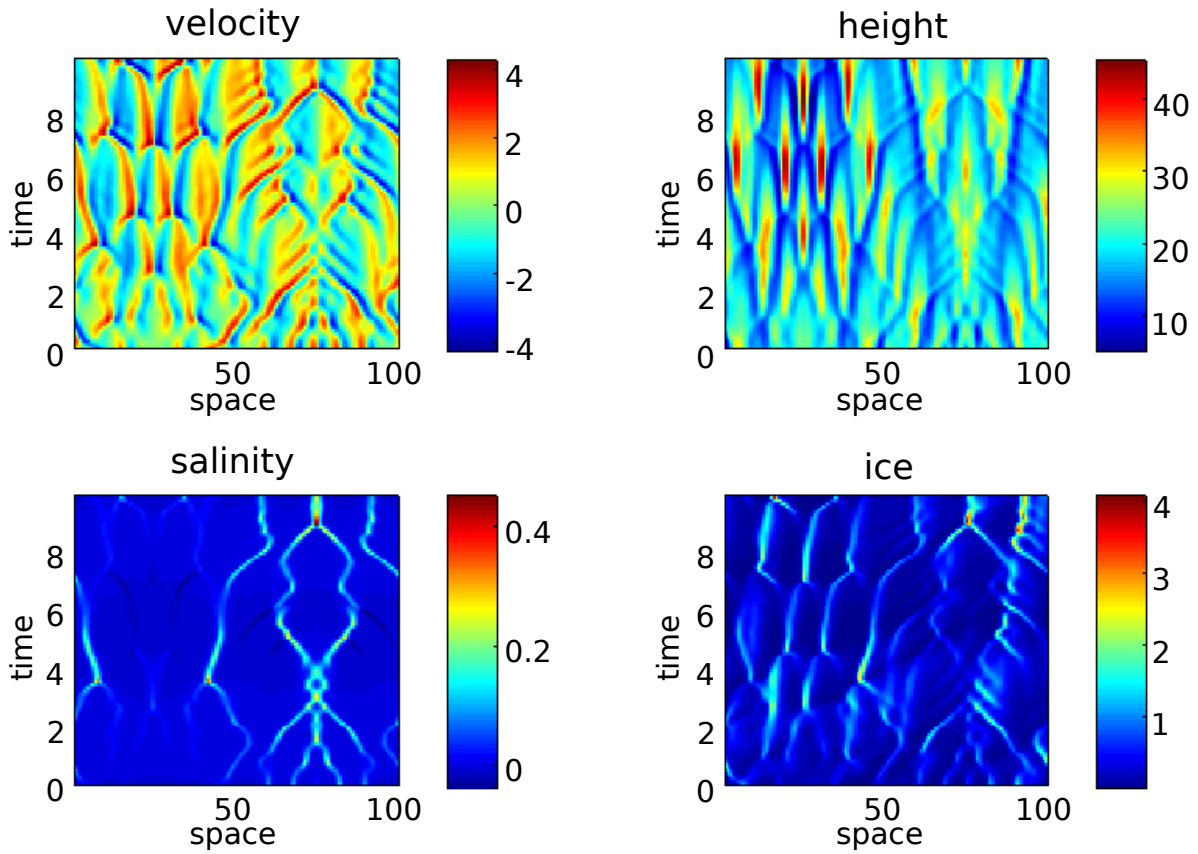

Figure 4: Free running simulation of the coupled multivariate model.

Table 3: Lowest RMS error for different assimilation schemes and the corresponding parameters for salinity.

	L	inflation	mean RMS	std of mean RMS
CL	17	1.00	0.18362	0.00070
CL-adj	7	1.02	0.18228	0.00047
LEnKF-pert	17	1.02	0.17444	0.00063
CLEnKF-pert	17	1.02	0.17254	0.00064
LEnKF $\mathbf{P}_c$	17	1.02	0.18689	0.00080
CLEnKF $\mathbf{P}_c$	17	1.02	0.18549	0.00080
LEnKF $\mathbf{S}\mathbf{S}^T$	17	1.02	0.17244	0.00064
CLEnKF $\mathbf{S}\mathbf{S}^T$	17	1.02	**0.17064**	0.00065

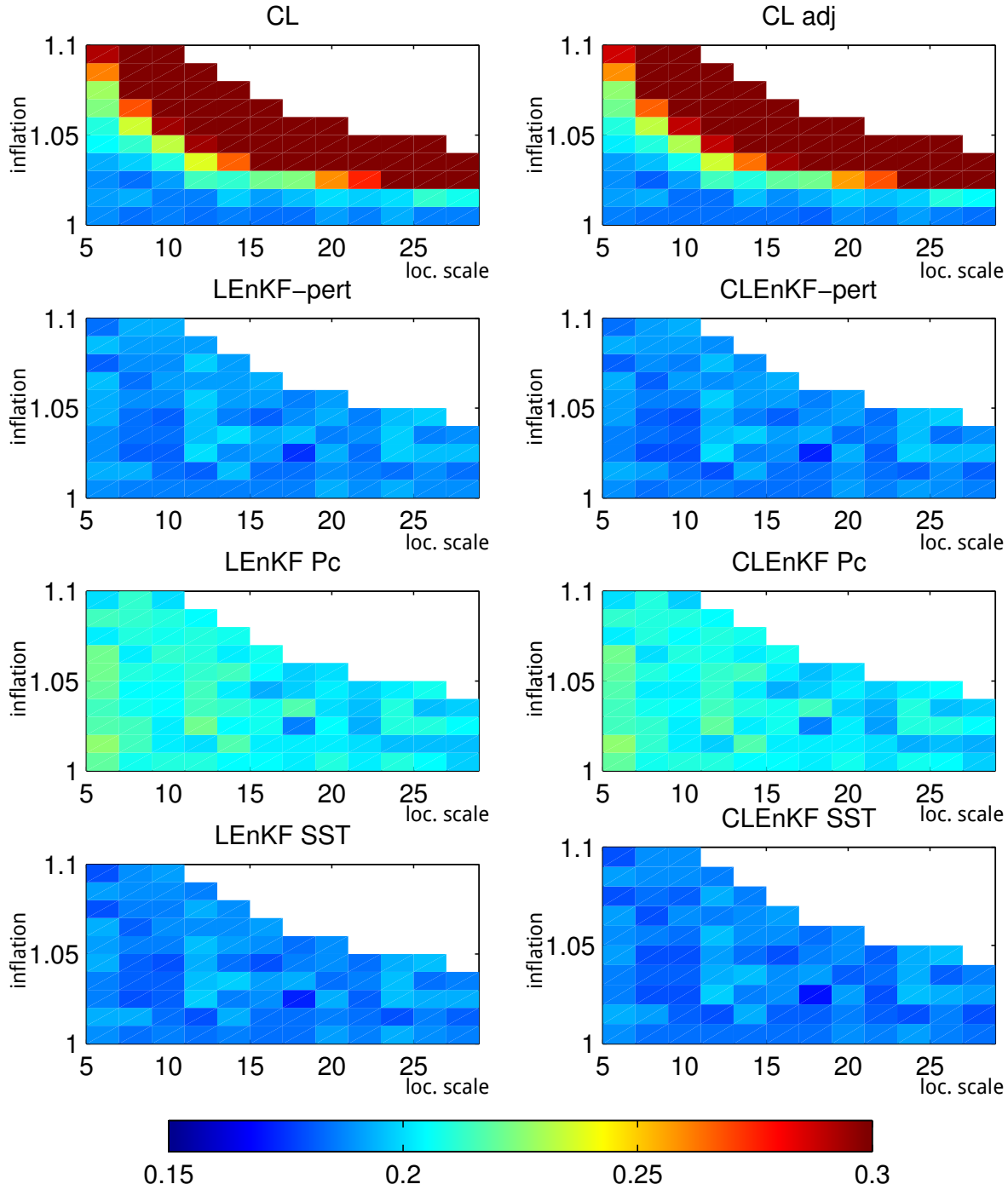

Figure 5: RMS error between the model run with assimilation and the true solution for different schemes and parameters.

5 Conclusions

This study presented three new local assimilation schemes which are formulated globally (i.e. for the whole state vector) where spurious long-range correlations can be filtered out and global conservation properties can be enforced. In principle, non-local observation operators can be used (e.g. assimilation of observation representing an average). Twin experiments with Kuramoto-Sivashinsky and a simple model mimicking the coupling between salinity and sea ice show the benefit of this approach compared to the traditional covariance localization scheme where observations are assimilated sequentially.

Different variants of this approach were discussed (stochastic scheme, deterministic scheme, deterministic scheme avoiding potential rotation of the error space). In general it was shown that the inclusion of the conservation property is beneficial to reduce the total RMS error. For the tested cases, the stochastic scheme and deterministic scheme avoiding error space rotation provided better results than the standard covariance localization where observations are assimilated sequentially. Which variant of the schemes provides the best results depended in fact on the tested model. But as a general conclusion, one can recommend the scheme CLEnKF-$\mathbf{S}\mathbf{S}^T$ which was the second best scheme for the univariate model and the best scheme for the multivariate model.

This study may open future research perspectives. For instance, the presented approaches could be extended to a local assimilation scheme where uncertainties in the conserved quantity are allowed and the analysis update is consistent with this uncertainty. The presented schemes would then just be a special case of this extended approach.

Acknowledgments

This work was funded by the SANGOMA EU project (grant FP7-671 SPACE-2011-1-CT-283580-SANGOMA), by the project PREDANTAR (SD/CA/04A) from the federal Belgian Science policy and the Fonds de la Recherche Scientifique de Belgique (F.R.S.-

FNRS). Computational resources have been provided by the Consortium des Équipements de Calcul Intensif (CÉCI), funded by the Fonds de la Recherche Scientifique de Belgique (F.R.S.-FNRS) under Grant No. 2.5020.11. We would like to thank the reviewers and the editor for their careful reading of the manuscript and their constructive criticism.

References

Anderson JL (2007) Exploring the need for localization in ensemble data assimilation using a hierarchical ensemble filter. Physica D: Nonlinear Phenomena 230(1-2):99–111, doi:10.1016/j.physd.2006.02.011

Barth A, Alvera-Azcárate A, Beckers JM, Rixen M, Vandenbulcke L (2007) Multigrid state vector for data assimilation in a two-way nested model of the Ligurian Sea. Journal of Marine Systems 65(1-4):41–59, doi:10.1016/j.jmarsys.2005.07.006, URL http://hdl.handle.net/2268/4260

Barth A, Beckers JM, Troupin C, Alvera-Azcárate A, Vandenbulcke L (2014) divand-1.0: n-dimensional variational data analysis for ocean observations. Geoscientific Model Development 7(1):225–241, doi:10.5194/gmd-7-225-2014, URL http://www.geosci-model-dev.net/7/225/2014/

Bishop CH, Hodyss D (2007) Flow-adaptive moderation of spurious ensemble correlations and its use in ensemble-based data assimilation. Quarterly Journal of the Royal Meteorological Society 133(629):2029–2044, doi:10.1002/qj.169

Bishop CH, Hodyss D (2009a) Ensemble covariances adaptively localized with ECO-RAP. Part 1: tests on simple error models. Tellus A 61(1):84–96, doi:10.1111/j.1600-0870.2008.00371.x

Bishop CH, Hodyss D (2009b) Ensemble covariances adaptively localized with ECO-RAP. Part 2: a strategy for the atmosphere. Tellus A 61(1):97–111, doi:10.1111/j.1600-0870.2008.00372.x

Bishop CH, Hodyss D (2011) Adaptive Ensemble Covariance Localization in Ensemble 4D-VAR State Estimation. Monthly Weather Review 139:1241–1255, doi:10.1175/2010MWR3403.1

Bishop CH, Etherton B, Majumdar SJ (2001) Adaptive Sampling with the Ensemble Transform Kalman Filter. Part I: Theoretical Aspects. Monthly Weather Review 129:420–436, doi:10.1175/1520-0493(2001)129⟨0420:ASWTET⟩2.0.CO;2

Brankart JM, Testut CE, Brasseur P, Verron J (2003) Implementation of a multivariate data assimilation scheme for isopycnic coordinate ocean models: application to a 1993-96 hindcast of the North Atlantic Ocean circulation. Journal of Geophysical Research 108(C3):3074, doi:10.1029/2001JC001198

Brankart JM, Ubelmann C, Testut CE, Cosme E, Brasseur P, Verron J (2009) Efficient Parameterization of the Observation Error Covariance Matrix for Square Root or Ensemble Kalman Filters: Application to Ocean Altimetry. Monthly Weather Review 137:1908–1927, doi:10.10.1175/2008MWR2693.1

Burgers G, van Leeuwen PJ, Evensen G (1998) Analysis scheme in the ensemble Kalman filter. Monthly Weather Review 126:1719–1724, doi:10.1175/1520-0493(1998)126⟨1719:ASITEK⟩2.0.CO;2

Chen Y, Davis TA, Hager WW, Rajamanickam S (2008) Algorithm 887: Cholmod, supernodal sparse cholesky factorization and update/downdate. ACM Transactions on Mathematical Software 35(3):22:1–22:14, doi:10.1145/1391989.1391995

Cox S, Matthews P (2002) Exponential time differencing for stiff systems. Journal of Computational Physics 176(2):430 – 455, doi:10.1006/jcph.2002.6995

Danilov S (2013) Ocean modeling on unstructured meshes. Ocean Modelling 69:195 – 210, doi:10.1016/j.ocemod.2013.05.005

552 Davis TA, Hager WW (2009) Dynamic supernodes in sparse Cholesky update/downdate
553 and triangular solves. ACM Transactions on Mathematical Software 35(4):27:1–27:23,
554 doi:10.1145/1462173.1462176

555 Evensen G (2007) Data assimilation: the Ensemble Kalman Filter. Springer, 279pp

556 Gaspari G, Cohn SE (1999) Construction of correlation functions in two and three di-
557 mensions. Quarterly Journal of the Royal Meteorological Society 125(554):723–757,
558 doi:10.1002/qj.49712555417

559 Greybush SJ, Kalnay E, Miyoshi T, Ide K, , Hunt BR (2011) Balance and Ensemble
560 Kalman Filter Localization Techniques. Monthly Weather Review 139:511–522, doi:
561 10.1175/2010MWR3328.1

562 Hamill TM, Whitaker JS, Snyder C (2001) Distance-dependent filtering of background
563 error covariance estimates in an ensemble Kalman filter. Monthly Weather Review
564 129:2776–2790, doi:10.1175/1520-0493(2001)129⟨2776:DDFOBE⟩2.0.CO;2

565 Hoteit I, Pham DT, Blum J (2002) A simplified reduced order Kalman filtering and ap-
566 plication to altimetric data assimilation in Tropical Pacific. Journal of Marine Systems
567 36:101–127, doi:10.1016/S0924-7963(02)00129-X

568 Houtekamer PL, Mitchell HL (1998) Data assimilation using ensemble Kalman filter tech-
569 nique. Monthly Weather Review 126:796–811, doi:10.1175/1520-0493(1998)126⟨0796:
570 DAUAEK⟩2.0.CO;2

571 Houtekamer PL, Mitchell HL (2001) A sequential ensemble Kalman filter for atmospheric
572 data assimilation. Monthly Weather Reviev 129:123–137, doi:10.1175/1520-0493(2001)
573 129⟨0123:ASEKFF⟩2.0.CO;2

574 Hunt BR, Kostelich EJ, Szunyogh I (2007) Efficient data assimilation for spatiotemporal
575 chaos: A local ensemble transform Kalman filter. Physica D 230:112–126, doi:10.1016/
576 j.physd.2006.11.008

577 Ide K, Bennett P, Courtier M, Ghil M, Lorenc AC (1995) Unified notation for data
578 assimilation: Operational, sequential and variational. Journal of the Meteorological
579 Society of Japan 75(1B):181–189

580 Janjić T, Nerger L, Albertella A, Schröter J, Skachko S (2011) On domain localization in
581 ensemble based Kalman filter algorithms. Monthly Weather Review 139(7):2046–2060,
582 doi:10.1175/2011MWR3552.1

583 Janjić T, McLaughlin DB, Cohn SE (2012) Preservation of physical properties with en-
584 semble based Kalman filter algorithms. In: Mathematical and Algorithmic Aspects of
585 Atmosphere-Ocean Data Assimilation, Mathematisches Forschungsinstitut Oberwol-
586 fach, 58, pp 17–20, doi:10.4171/OWR/2012/58

587 Janjić T, McLaughlin D, Cohn SE, Verlaan M (2014) Conservation of mass and preser-
588 vation of positivity with ensemble-type Kalman filter algorithms. Monthly Weather
589 Review 142:755–773, doi:10.1175/MWR-D-13-00056.1

590 Kepert JD (2009) Covariance localisation and balance in an Ensemble Kalman Fil-
591 ter. Quarterly Journal of the Royal Meteorological Society 135(642):1157–1176, doi:
592 10.1002/qj.443

593 Keppenne CL, Rienecker MM (2003) Assimilation of temperature into an isopycnal ocean
594 general circulation model using a parallel ensemble Kalman filter. Journal of Marine
595 Systems 40-41:363 – 380, doi:10.1016/S0924-7963(03)00025-3

596 Khellat F, Vasegh N (2014) The Kuramoto–Sivashinsky equation revisited: Low-
597 dimensional corresponding systems. Communications in Nonlinear Science and Nu-
598 merical Simulation 19(9):3011 – 3022, doi:10.1016/j.cnsns.2014.01.015

599 Lorenc AC (2003) The potential of the ensemble Kalman filter for NWP—a comparison
600 with 4D-Var. Quarterly Journal of the Royal Meteorological Society 129(595):3183–
601 3203, doi:10.1256/qj.02.132

Löhner RD, Ambrosiano J (1990) A vectorized particle tracer for unstructured grids. Journal of Computational Physics 91(1):22 – 31, doi:10.1016/0021-9991(90)90002-I

Madec G (2014) NEMO ocean engine (Draft edition r6039). No. 27 in Note du Pôle de modélisation, Institut Pierre-Simon Laplace (IPSL), France

Moore AM, Arango HG, Broquet G, Powell BS, Weaver AT, Zavala-Garay J (2011) The Regional Ocean Modeling System (ROMS) 4-dimensional variational data assimilation systems: Part I - System overview and formulation. Progress in Oceanography 91(1):34 – 49, doi:10.1016/j.pocean.2011.05.004

Nerger L (2015) On Serial Observation Processing in Localized Ensemble Kalman Filters. Monthly Weather Review 143:1554–1567, doi:10.1175/MWR-D-14-00182.1

Nerger L, Hiller W (2013) Software for ensemble-based data assimilation systems-Implementation strategies and scalability. Computers & Geosciences 55:110 – 118, doi:10.1016/j.cageo.2012.03.026

Nerger L, Hiller W, Schröter J (2005) A Comparison of Error Subspace Kalman Filters. Tellus series A: Dynamic meteorology and oceanography 57A(5):715–735, doi:10.1111/j.1600-0870.2005.00141.x

Nerger L, Janjić T, Schröter J, Hiller W (2012a) A regulated localization scheme for ensemble-based kalman filters. Quarterly Journal of the Royal Meteorological Society 138(664):802–812, doi:10.1002/qj.945

Nerger L, Janjić T, Schröter J, Hiller W (2012b) A unification of ensemble square root kalman filters. Monthly Weather Review 140, doi:10.1175/MWR-D-11-00102.1

Pan M, Wood EF (2006) Data assimilation for estimating the terrestrial water budget using a constrained Ensemble Kalman Filter. J Hydrometeor 7:534–547, doi:10.1175/JHM495.1

626 Shchepetkin A, McWilliams J (2005) The Regional Oceanic Modeling System: A split-
627 explicit, free-surface, topography-following-coordinate ocean model. Ocean Modelling
628 9:347–404, doi:10.1016/j.ocemod.2004.08.002

629 Troupin C, Barth A, Sirjacobs D, Ouberdous M, Brankart JM, Brasseur P, Rixen M,
630 Alvera-Azcárate A, Belounis M, Capet A, Lenartz F, Toussaint ME, Beckers JM (2012)
631 Generation of analysis and consistent error fields using the Data Interpolating Vari-
632 ational Analysis (DIVA). Ocean Modelling 52–53:90–101, doi:10.1016/j.ocemod.2012.
633 05.002, URL http://hdl.handle.net/2268/125731

634 Wang Q, Zhou W, Wang D, Dong D (2013) Ocean model open boundary conditions with
635 volume, heat and salinity conservation constraints. Advances in Atmospheric Sciences
636 31(1):188–196, doi:10.1007/s00376-013-2269-y

637 Weaver AT, Courtier P (2001) Correlation modelling on the sphere using a generalized
638 diffusion equation. Quarterly Journal of the Royal Meteorological Society 127:1815–
639 1842, doi:10.1002/qj.49712757518

640 Weaver AT, Vialard J, Anderson DLT (2003) Three- and Four-Dimensional Variational
641 Assimilation with a General Circulation Model of the Tropical Pacific Ocean. Part I:
642 Formulation, Internal Diagnostics, and Consistency Checks. Monthly Weather Review
643 131:1360–1378, doi:10.1175/1520-0493(2003)131⟨1360:TAFVAW⟩2.0.CO;2

644 Whitaker JS, Hamill TM (2002) Ensemble data assimilation without perturbed obseva-
645 tions. Monthly Weather Review 130:1913–1924, doi:10.1175/1520-0493(2002)130⟨1913:
646 EDAWPO⟩2.0.CO;2

647 White L, Legat V, Deleersnijder E (2008) Tracer Conservation for Three-Dimensional,
648 Finite-Element, Free-Surface, Ocean Modeling on Moving Prismatic Meshes. Monthly
649 Weather Review 136:420–442, doi:10.1175/2007MWR2137.1

650 Zhu J, Zheng F, Li X (2011) A new localization implementation scheme for ensemble

data assimilation of non-local observations. Tellus A 63(2), doi:10.1111/j.1600-0870.2010.00486.x

A Preconditioning

In order to accelerate the convergence of the conjugate gradient method, a preconditioner matrix $\mathbf{T}$ is applied, which transforms the equation (14) into:

$$\mathbf{T}^{-1}\mathbf{A}\mathbf{z} = \mathbf{T}^{-1}\mathbf{b}. \tag{51}$$

A preconditioner is efficient if one can quickly compute $\mathbf{T}^{-1}\mathbf{z}$ for any vector $\mathbf{z}$ and if the product $\mathbf{T}^{-1}\mathbf{A}$ is better conditioned than the matrix $\mathbf{A}$. Different choices of the preconditioner matrix are possible. For instance, one can derive a preconditioner based on the global analysis problem which can be solved very efficiently using the Sherman-Morrison-Woodbury formula (for diagonal $\mathbf{R}$). In this case, the preconditioner is defined as

$$\mathbf{T} = \mathbf{R} + \mathbf{HS}(\mathbf{HS})^T, \tag{52}$$

and its inverse is given by

$$\mathbf{T}^{-1} = \mathbf{R}^{-1} - \mathbf{R}^{-1}\mathbf{HS}\left(\mathbf{I} + (\mathbf{HS})^T\mathbf{R}^{-1}\mathbf{HS}\right)^{-1}(\mathbf{HS})^T\mathbf{R}^{-1}. \tag{53}$$

Without localization, $\mathbf{T}$ would be equal to $\mathbf{A}$ and the preconditioned conjugate gradient algorithm would converge in just one iteration. This is a suitable preconditioner if in equation (9), the structure of $\mathbf{P}'$ is essentially determined by the ensemble covariance matrix $\mathbf{P}$. If however the structure of $\mathbf{P}'$ is essentially given by the localization matrix $\boldsymbol{\rho}$, then one could choose:

$$\mathbf{T} = \mathbf{R} + \mathbf{H}\boldsymbol{\rho}\mathbf{H}^T \tag{54}$$

$$\mathbf{T}^{-1} = \mathbf{R}^{-1} - \mathbf{R}^{-1}\mathbf{H}\boldsymbol{\rho}^a\mathbf{H}^T\mathbf{R}^{-1}, \tag{55}$$

where

$$\boldsymbol{\rho}^a = \left(\boldsymbol{\rho}^{-1} + \mathbf{H}^T\mathbf{R}^{-1}\mathbf{H}\right)^{-1}, \tag{56}$$

which can be solved efficiently if $\boldsymbol{\rho}$ is approximated by a diffusion operator and its square root decomposition is readily available (*e.g.* Weaver and Courtier, 2001; Weaver et al, 2003; Moore et al, 2011) or if $\boldsymbol{\rho}^{-1}$ is expressed as a sparse matrix as in the spline interpolation (*e.g.* Troupin et al, 2012; Barth et al, 2014) and using efficient sparse matrix solvers (*e.g.* Chen et al, 2008; Davis and Hager, 2009). In the latter case, it is also worth to mention that the most CPU time-consuming step is the Cholesky factorization of the matrix $\boldsymbol{\rho}^{-1} + \mathbf{H}^T\mathbf{R}^{-1}\mathbf{H}$ which needs to be done only once per assimilation cycle.

Effectively, in the first case (equation (52)) one uses the solution of the global analysis as a preconditioner. In the second case, one would use the 3D-Var algorithm as a preconditioner (equation (55)). The matrix $\boldsymbol{\rho}^a$ can in fact be interpreted as the posterior error covariance matrix of the variational problem assuming that the prior error covariance is equal to the localization function.